

Investigation of Blend Miscibility of a Ternary PS/PCHMA/PMMA System Using SIMS and Mean-Field Theory

Shane E. Harton,[†] Tadanori Koga,[‡] Frederick A. Stevie,[§] Tohru Araki,[⊥] and Harald Ade^{*,⊥}

Department of Materials Science & Engineering, North Carolina State University, Raleigh, North Carolina 27695; Department of Materials Science & Engineering, Stony Brook University, Stony Brook, New York 11794; Analytical Instrumentation Facility, North Carolina State University, Raleigh, North Carolina 27695; and Department of Physics, North Carolina State University, Raleigh, North Carolina 27695

Received July 21, 2005; Revised Manuscript Received October 11, 2005

ABSTRACT: Poly(cyclohexyl methacrylate) (PCHMA) and polystyrene (PS) are miscible with each other, but each is highly immiscible with PMMA. Identifiable by the asymmetries in the binary mean-field interaction parameters χ , PS preferentially segregates to the PCHMA/PMMA interface. Secondary ion mass spectrometry was used to provide real-space depth profiles of deuterated PS (dPS) in a miscible blend with PCHMA. The initial dPS concentration was varied from 5 to 20% (v/v), and the blend film was annealed at 150 °C on a film of PMMA for 42 h. X-ray reflectometry was used to determine the interfacial width between PCHMA and PMMA at 150 °C. Using self-consistent mean-field theory, good agreement was found between the experimental and theoretical interfacial excess Z^* of dPS at each concentration. Because of their similar glass transition temperatures (~ 100 °C for PS and PCHMA) and the ability of PS and PCHMA to be controllably synthesized with low polydispersities, we anticipate this blend to be a model system for future investigations of such phenomena as diffusion in miscible blends and diffusion near surfaces and interfaces.

Introduction

Miscible polymer blends have been model systems for investigation of polymer dynamics^{1–6} and equilibrium segregation at polymer surfaces^{7–9} and polymer/polymer interfaces.^{10,11} They are often composed of polymer pairs that have an apparent exothermic enthalpy of mixing.^{1,7,12–14} Characterized by a lower critical solution temperature (LCST) type phase behavior, these systems are miscible at low temperatures when $\chi_{AB} < 0$, where χ_{AB} is the mean-field enthalpic interaction parameter between homopolymers A and B,¹⁵ and tend to phase separate as they are heated above the critical temperature (T_c). This type of phase behavior can often be attributed to specific interactions, such as hydrogen bonding,¹⁶ or large differences in polymer free-volume.¹⁷ Previously investigated binary LCST blends have included polystyrene (PS) in combination with poly(xylenyl ether) (PXE),^{1,14} poly(vinyl methyl ether) (PVME),^{7,18} or tetramethylbisphenol A polycarbonate (TMPC).^{12,13} Although these systems have been employed for investigations of such phenomena as surface segregation⁷ and mutual or self-diffusion,^{1,12–14} they suffer from highly asymmetric glass transition temperatures (T_g 's). These asymmetries can lead to spatially varying T_g 's and polymer chains possessing significantly different monomeric friction coefficients,^{13,14} making accurate decoupling of various phenomena extremely difficult.^{4–6} The need for a model LCST system involving polymers with similar T_g 's and well-defined thermody-

namic parameters has motivated the present investigation.

Polymer blend phase behavior changes dramatically near surfaces and interfaces due to a reduction in conformational entropy,¹⁹ and asymmetries in χ_{AC} and χ_{BC} can lead to segregation of an A polymer to an A:B/C interface,^{10,11,20,21} where A and B are miscible with each other, yet each is immiscible with C. An extremely powerful theoretical method for analyzing these types of systems is self-consistent mean-field theory (SCMF).¹⁹ Even though it is computationally much less costly than detailed numerical simulations,²² SCMF has been found to produce accurate representation of polymer interfaces within the mean-field limit.²³ Because of its accuracy and low computational cost, it can be used to determine χ from such experimental measurements as interfacial width w ²⁴ and interfacial segregation.²⁵

Secondary ion mass spectrometry (SIMS) is a widely used experimental technique for obtaining depth profiles of tracer-labeled polymers.²⁶ With its high depth resolution, it can be used to quantify an interfacial excess,^{27,28} surface excess,²⁹ and diffusion gradient³⁰ of a labeled polymer in a polymer film. Even with the superb depth resolution attainable using SIMS, it is extremely difficult to measure w for systems where w is smaller than the instrumental resolution.³¹ For this situation, X-ray or neutron reflectometry^{32,33} (XR or NR, respectively) can complement SIMS.²⁶ In this article, we present direct measurements of the interfacial excess Z^* of deuterated polystyrene (dPS) at the interface between poly(cyclohexyl methacrylate) (PCHMA) and poly(methyl methacrylate) (PMMA) as a function of dPS concentration in PCHMA using SIMS. XR is used to determine w between PCHMA and PMMA. SCMF is used to theoretically analyze Z^* and the changes in w and interfacial tension γ as a function of dPS concentration in PCHMA. The potential applications of the PS/

[†] Department of Materials Science & Engineering, North Carolina State University.

[‡] Stony Brook University.

[§] Analytical Instrumentation Facility, North Carolina State University.

[⊥] Department of Physics, North Carolina State University.

* Corresponding author: e-mail harald_ade@ncsu.edu.

PCHMA and PS/PCHMA/PMMA systems for model investigations of polymer diffusion and dynamics are outlined.

Experimental Section

Materials and Sample Preparation. Atactic dPS (polymer A) ($M_w = 76.6$ kDa; $M_w/M_n = 1.05$) was purchased from Polymer Source. Atactic PCHMA (polymer B) and syndiotactic PMMA (polymer C) ($M_w = 101.0$ kDa; $M_w/M_n = 1.09$) were purchased from Scientific Polymer Products. For PCHMA, the viscosity average molecular weight M_v was determined to be 74 kDa using dilute solution viscometry in 1-butanol at 22.5 °C (T_θ).³⁴ The inflection-point T_g 's of dPS, PCHMA, and PMMA were determined to be 97, 102, and 127 °C, respectively, using differential scanning calorimetry (cooling cycle of 10 °C/min).

Silicon (100) wafers were cut into 2.5 cm \times 2.5 cm squares and cleaned according to established procedures.³⁰ Immediately prior to spin-casting, they were soaked in hydrofluoric acid (~10% v/v in water) for 1 min and washed with deionized water. PMMA was cast onto the H-passivated Si from toluene and annealed for 1 h at 150 °C to remove residual solvent and create smooth surfaces. For SIMS analysis dPS/PCHMA films were cast from 1-chloropentane directly onto the PMMA layer and annealed at 150 °C for 42 h. The dPS concentration in the film was varied from 5 to 20% (v/v). These samples had a PMMA layer thickness of 95 nm and a dPS/PCHMA layer thickness of 125 nm as measured using ellipsometry. Films of the dPS/PCHMA blend were also cast onto Si wafers possessing a native oxide layer (~2 nm) and floated onto TEM grids from deionized water. Scanning transmission X-ray microscopy (STXM) at beamline 5.3.2 at the Advanced Light Source in Berkeley^{35,36} confirms that no phase separated domains larger than ~25 nm (minimum resolvable domain size) were present in the as-cast dPS/PCHMA layers. Two characteristic photon energies, the PS phenyl ring $\pi^*_{C=C}$ peak energy (~285.2 eV) and PCHMA carbonyl $\pi^*_{C=O}$ peak energy (~288.4 eV), were used in the STXM analyses. Because of absence of an observable morphology, the STXM results are not included here explicitly. For XR analysis, PCHMA was cast onto PMMA from 1-chloropentane and annealed for 24 h at 150 °C. Single-layer PMMA and PCHMA films were also prepared to determine the X-ray dispersions δ of the two polymers.

Secondary Ion Mass Spectrometry. The deuterium depth profiles were acquired using a CAMECA IMS-6f magnetic sector spectrometer using a 15 nA Cs⁺ primary beam (6.0 keV impact energy) rastered over a 200 μ m \times 200 μ m area with detection of negative secondary ions from a 60 μ m diameter circle at the center. A sacrificial PS top layer (50 nm) was added after the 42 h anneal to ensure that the preequilibrium distance (range of bombarding species) was sputtered away before the layer of interest was reached, and a 20 nm gold coating was deposited on top of the sacrificial layer to minimize sample charging. The analysis conditions used provide a nominal depth resolution of ~8–10 nm. Some analyses were also made using O₂⁺ at 5.5 keV impact energy, but the results showed poorer depth resolution than the Cs⁺ data for the structure analyzed.

X-ray Reflectometry. The XR measurements have been carried out at beamline X10B at the National Synchrotron Light Source (NSLS), Brookhaven National Laboratory (BNL), using a photon energy of 14 keV (i.e., X-ray wavelength $\lambda = 0.87$ Å). The specularly reflected intensity was measured by varying α_i and α_f while maintaining $\alpha_i = \alpha_f$ (α_i and α_f are the incident and reflected angles, respectively). Because the specular reflectivity, presented as scattered intensity vs scattering vector $q_z = (4\pi/\lambda) \sin \alpha_i$, detects the variation of the electron density in the direction normal to the surface, it is sensitive to film thickness h , density ρ , interfacial width w , and surface roughness σ . However, in the case of XR analysis of polymer bilayer systems, difficulties often arise in obtaining details regarding polymer–polymer interfaces due to the small X-ray contrast $\Delta\delta/\delta$ between the individual polymers,³² which is typically less than 10% for most polymer pairs.³³ To overcome this difficulty, we used a Fourier transformation (FT) analysis

Table 1. Reported Values of χ for dPS/PMMA, PS/PCHMA, and PCHMA/PMMA at 150 °C

polymer pair	χ (150 °C)
dPS/PMMA ⁴¹	0.038
PS/PCHMA (1) ³⁷	−0.0034
PS/PCHMA (2) ³⁸	−0.015
PCHMA/PMMA ³⁸	0.097

Table 2. XR Analysis of PCHMA and PMMA Single-Layer Films

	h/nm	σ/nm	a/nm	$\delta \times 10^6$
PCHMA	72.5	0.28	0.73 ³⁴	1.24
PMMA	61.7	0.43	0.65 ³⁹	1.21

method developed previously.³² A four-layer model (i.e., Si substrate, native oxide layer, PMMA layer, and PCHMA layer) was used to fit the XR data.

Results and Discussion

Table 1 shows the χ values for the three binary interactions at 150 °C. Note the two different values that have been reported for PS/PCHMA.^{37,38} To analyze the PCHMA/PMMA bilayers with XR, single layers of PCHMA and PMMA were used to measure the dispersion δ of the two polymers individually. Those values, along with the statistical segment lengths a ,^{34,39} h , and σ , are listed in Table 2. Using the measured values for δ , the PCHMA/PMMA bilayers were analyzed using the FT method,³² as shown in Figure 1, and w_{BC} was determined to be 1.6 nm. It should be noted that the X-ray contrast between PCHMA and PMMA is quite small (<3%), and the value for w_{BC} is considered a lower limit. From the analytical solution of SCMF for w_{BC} ⁴⁰

$$w_{BC} = \left(\frac{a_B^2 + a_C^2}{3\chi_{BC}} \right)^{1/2} \quad (1)$$

χ_{BC} was approximated to be 0.1, in agreement with prior results (see Table 1).³⁸

Using SIMS, the interfacial excess of dPS at the PCHMA/PMMA interface was determined for initial dPS concentrations of 5, 10, and 20% (v/v) in PCHMA, as shown in Figure 2. The convoluted dPS profiles were fit to a Gaussian error function for the surface and equilibrium dPS in the PCHMA layer and a Gaussian peak for the segregated dPS at the interface.²⁷ The interfacial excess is determined from the expression

$$Z^* \equiv \left(\frac{\pi}{4 \ln 2} \right)^{1/2} \varphi_p \Delta \quad (2)$$

where φ_p is the height and Δ is the full width at half-maximum of the Gaussian peak. The full width at half-maximum of the error function is used as a measure of the instrumental resolution, which is ~8–10 nm for this system under these analysis conditions. As shown in Figure 3, the use of Cs⁺ primary ions provides improved depth resolution when compared with bombardment using 5.5 keV impact energy O₂⁺ primary ions for this system. Using eq 2, Z^*/R was determined to be 0.053, 0.055, and 0.068 for initial concentrations of dPS of 5, 10, and 20%, respectively, where R is the rms end-to-end distance¹⁵ of a dPS chain ($R \approx 18$ nm). The rms error for each measurement is ~5–10%.

The χ parameters for PS/PCHMA,^{37,38} PCHMA/PMMA,³⁸ and dPS/PMMA⁴¹ (χ_{AB} , χ_{BC} , and χ_{AC} , respectively) have been reported previously as a function of temperature. The χ for PCHMA/PMMA determined

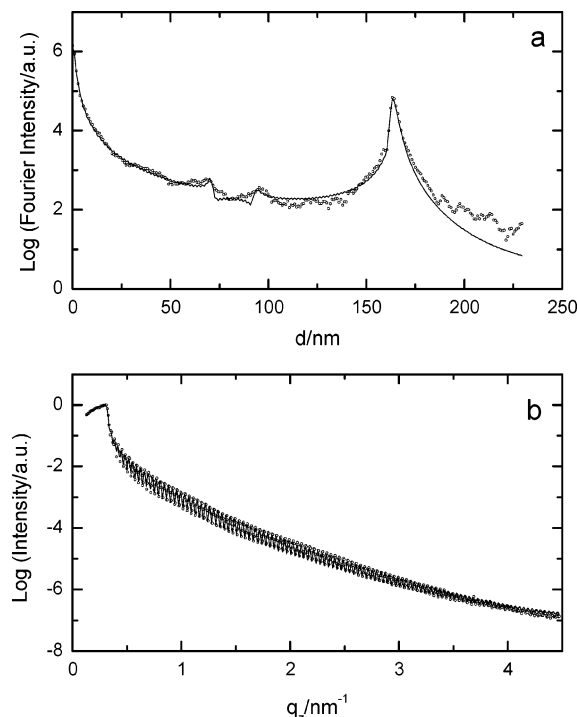


Figure 1. XR of PCHMA/PMMA (B/C) bilayers. The Fourier method (a) was used to determine the interfacial width of this low contrast system (see Table 2). The low contrast is observed in the reflectivity profile (b). Using eq 1, χ_{BC} was approximated to be 0.1.

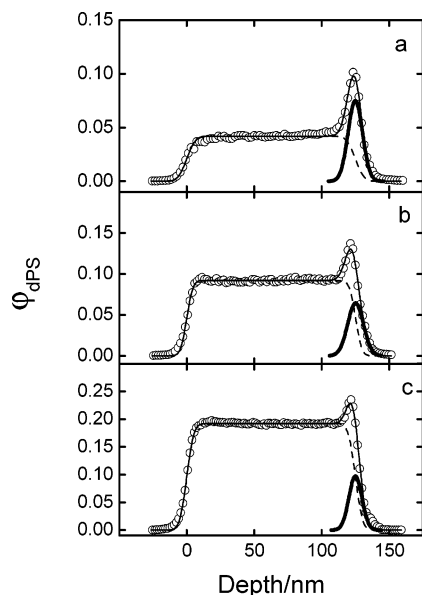


Figure 2. SIMS profiles for bilayers of dPS in PCHMA on PMMA (A:B/C) with (a) 5, (b) 10, and (c) 20% (v/v) initial concentrations of dPS. After depletion of dPS due to segregation to the interface during the 42 h anneal at 150 °C, the bulk concentration away from the interface (ϕ_A^∞) was reduced to (a) 4.3, (b) 9.2, and (c) 19.2%. The interfacial excess (Z^*) was determined from eq 2 after fitting the SIMS profiles to a Gaussian error function (dotted line) and a Gaussian peak (bold line) which superimpose to represent the convoluted dPS profile (solid line).²⁷

using XR ($\chi_{BC} \approx 0.1$) is almost identical to the reported value at 150 °C.³⁸ The measured χ_{BC} and the reported value of χ for dPS/PMMA at 150 °C ($\chi_{AC} = 0.038$)⁴¹ are used in the SCMF calculations. The corresponding

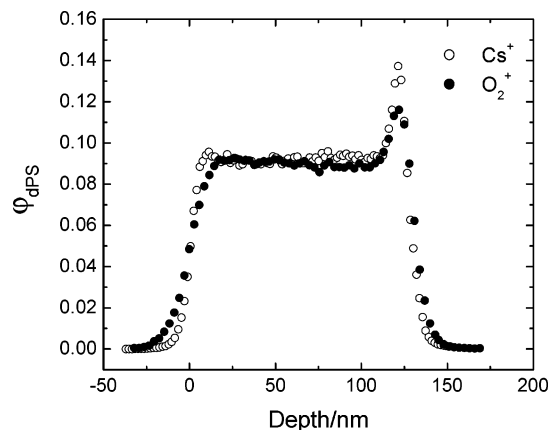


Figure 3. Comparison of Cs^+ (○) and O_2^+ (●) primary ion bombardment with 6.0 and 5.5 keV impact energies, respectively. For this system, Cs^+ clearly provides improved depth resolution.

highly incompatible interaction should drive the PCHMA away from the PMMA interface and lead to dPS segregation. Two significantly different values of χ for PS/PCHMA at 150 °C have been reported ($\chi_{AB} = -0.0034$ ³⁷ and -0.015 ,³⁸ as shown in Table 1), and the compatibility of each with the experimental measurements will be examined. Details of the equations and computational methods used in the SCMF calculations have been outlined elsewhere.^{11,20,21} Only the results are presented here for this ternary system of dPS/PCHMA on PMMA. A constant effective segment length ($a_e = 0.69 \text{ nm}$)⁴⁰ was used, where

$$a_e = \left(\frac{a_B^2 + a_C^2}{2} \right)^{1/2} \quad (3)$$

The effective segment length is almost identical to the segment length of PS ($a = 0.67 \text{ nm}$),³⁹ and the PS segmental volume (0.174 nm^3)⁴² is used as the reference volume. For simplicity, it was assumed that the number of segments was identical to that of dPS for all polymers ($N = 700$), and the polydispersity of PCHMA was neglected. Although polydispersity has been shown to have significant effects on polymer profiles at polymer/polymer interfaces,⁴³ the depth profiles for dPS, PCHMA, and PMMA should be dominated by enthalpic rather than entropic contributions,⁴⁴ because $\chi_{BC}N \sim 40$ (based on M_v of PCHMA) and there is a highly favorable interaction between dPS and PCHMA ($\chi_{AB}N \ll 0$).

Figure 4a shows an example of a simulated depth profile using $\chi_{AB} = -0.015$. The zero-point for the z -axis is set by the inflection point in the depth profile for C. To compare the SCMF calculations to the experimental data, the SCMF Z^* was calculated from

$$Z^* \equiv \int_{-\infty}^{\infty} [\phi_A - \phi_A^\infty(1 - \phi_C)] dz \quad (4)$$

where ϕ_A^∞ is the value of ϕ_A far from the interface (the depleted value for dPS), as demonstrated in Figure 4b. As shown in Figure 5, the value of $\chi_{AB} = -0.015$ provides much better agreement with the experimental measurements than $\chi_{AB} = -0.0034$, indicating that PS/PCHMA is indeed a highly miscible system at 150 °C, with $T_c \approx 225 \text{ °C}$.³⁸ Using $\chi_{AB} = -0.015$, the interfacial

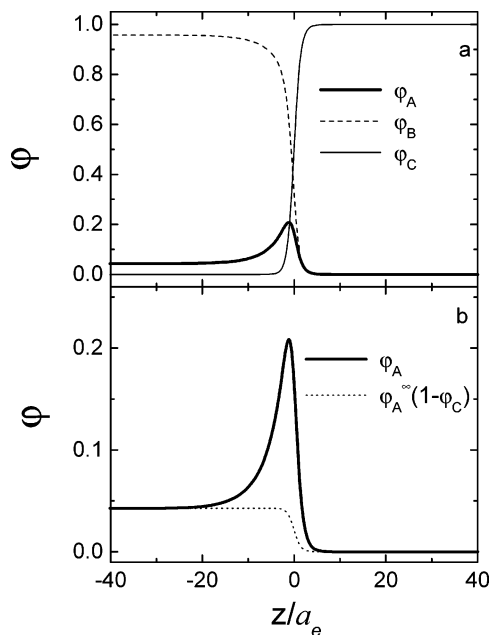


Figure 4. SCMF simulated profile for $\phi_A^\infty = 0.043$ (depleted dPS concentration for 5% initial concentration) using $\chi_{AB} = -0.015$, $\chi_{AC} = 0.038$, and $\chi_{BC} = 0.1$. Polymer A (dPS) is the bold line, polymer B (PCHMA) is the dotted line, and polymer C (PMMA) is the solid line in (a). Z^*/R was determined to be 0.044 from eq 4 and is the area between the bold and dotted lines in (b). Here, a_e is the effective segment length for B and C segments⁴⁰ from eq 3. The zero-point for the z -axis is set by the inflection point in the depth profile for C.

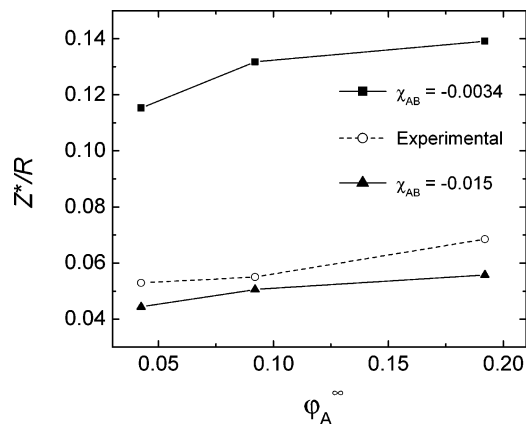


Figure 5. Interfacial excess (Z^*/R) measured from the SIMS profiles using eq 2 (○) as compared to SCMF calculations using $\chi_{AC} = 0.038$, $\chi_{BC} = 0.1$, and $\chi_{AB} = -0.0034$ (■) or -0.015 (▲). Lines are a guide for the eye. The theoretical values of Z^*/R were determined using eq 4. It is clear that $\chi_{AB} = -0.015$ provides far better representation of the experimental values than $\chi_{AB} = -0.0034$.

tensions γ_{ABC} and interfacial widths w_{ABC} have been calculated (see Figure 6) using^{11,20,21}

$$w_{ABC} = 4 \int_{-\infty}^{\infty} \phi_C (1 - \phi_C) dz \quad (5)$$

$$\gamma_{ABC} = kT\rho_0\zeta \int_{-\infty}^{\infty} (1 - \phi_A - \phi_B - \phi_C) dz \quad (6)$$

where kT is the thermal energy, ρ_0 is the lattice density, and ζ is a compressibility factor.¹⁹ For all of the calculations performed in this investigation, ζ was set to 8.0, which maintains high degree of incompressibility (i.e., $1 - \phi_A - \phi_B - \phi_C \sim 10^{-3}$).⁴⁵ These values are scaled

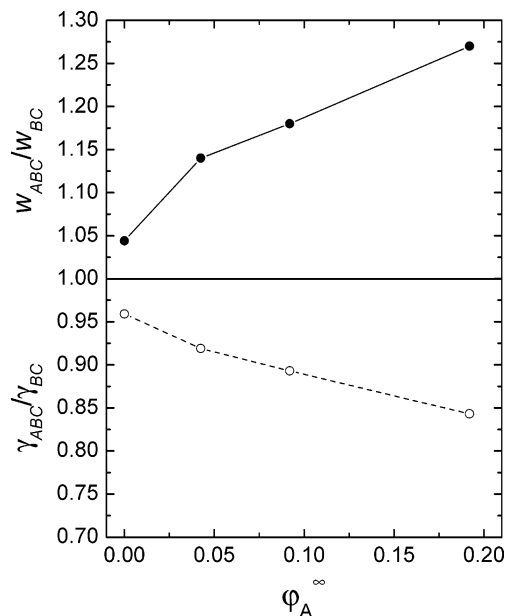


Figure 6. Interfacial width w_{ABC} (●) and interfacial tension γ_{ABC} (○) as determined using SCMF and eqs 5 and 6 with $\chi_{AB} = -0.015$, $\chi_{AC} = 0.038$, and $\chi_{BC} = 0.1$. Lines are a guide for the eye. Values are scaled to the infinite molecular weight w_{BC} and γ_{BC} from eqs 1 and 7,³⁴ respectively. Results are also shown for a numerical solution of a PCHMA/PMMA bilayer, where $\phi_A^\infty = 0$ ($N = 700$).

to w_{BC} (eq 1) and γ_{BC} in the limit of infinite molecular weight,⁴⁰ where

$$\gamma_{BC} = kT\rho_0 a_e \left(\frac{\chi_{BC}}{6} \right)^{1/2} \quad (7)$$

The seemingly low interfacial excess observed for dPS initial concentrations of 5–20% is due to the highly favorable interaction between dPS and PCHMA. This creates a powerful driving force to keep the dPS in the bulk.²¹ Although compatibilization does occur due to dPS segregation, from Figure 6 we see that the changes in γ_{ABC} and w_{ABC} are very small over this concentration range.

Because PS and PCHMA are so highly miscible over a large temperature range ($<225^\circ\text{C}$),³⁸ and the polymers have nearly identical T_g 's, this is indeed a model system for investigation of chain dynamics in miscible blends.^{4–6,37} We can also infer that, with known thermodynamic constants³⁸ and good agreement with SCMF (see Figure 5), the PS/PCHMA/PMMA ternary system would be ideal for investigation of potential driven diffusion near a bounding interface.^{46,47} Many of the polymers previously used for such investigations, such as PXE,^{1,14} PVME,^{7,18} and TMPC,^{12,13} are extremely difficult to controllably synthesize,⁴⁸ often resulting in somewhat high polydispersities ($M_w/M_n > 2$). Future investigations would be greatly improved through the use of a polymer system with each of the polymers having a low polydispersity ($M_w/M_n < 1.2$). PS and PMMA are well-known for their ability to be controllably synthesized with a low polydispersity,⁴⁹ but PCHMA has also been synthesized with techniques such as anionic³⁷ and controlled-radical^{50,51} polymerizations. These polymerization techniques have resulted in $M_w/M_n < 1.2$,⁴⁹ but unlike the synthesis of PMMA, the choice of method (radical or anionic) does not strongly influence the T_g of PCHMA.^{37,51,52}

Conclusions

We have presented an investigation of the segregation of dPS to an interface between highly immiscible PCHMA and PMMA. With SIMS, we have measured Z^*/R of 0.053, 0.055, and 0.068 for 5, 10, and 20% initial concentrations, respectively, of dPS in the PCHMA layer after 42 h at 150 °C. Using XR, the interfacial width between PCHMA and PMMA has been determined to be 1.6 nm at 150 °C. Calculated values of Z^*/R from SCMF calculations have shown good agreement with the experimental values of Z^*/R at all three concentrations using the reported value of χ for PS/PCHMA of -0.015^{38} rather than -0.0034^{37} . SCMF calculations also show that, because PS and PCHMA are so highly miscible, there is little change in w_{ABC} and γ_{ABC} over the concentration range employed here due to relatively low dPS segregation. We anticipate PS/PCHMA and PS/PCHMA/PMMA to be model systems for future investigations of such phenomena as diffusion in miscible blends^{13,14} and diffusion near interfaces^{46,47} by minimizing problems associated with asymmetric T_g 's of the polymer constituents.⁴⁻⁶

Acknowledgment. This work was supported by the National Science Foundation (DMR-0071743) and the U.S. Department of Energy (DE-FG02-98ER45737). XR measurements have been carried out at beamline X10B at the National Synchrotron Light Source. STXM measurements were performed with the polymer STXM at beamline 5.3.2 of the Advanced Light Source.

References and Notes

- Composto, R. J.; Mayer, J. W.; Kramer, E. J.; White, D. M. *Phys. Rev. Lett.* **1986**, *57*, 1312.
- Brochard, F.; Jouffroy, J.; Levinson, P. *Macromolecules* **1983**, *16*, 1638.
- Brochard, F.; Jouffroy, J.; Levinson, P. *Macromolecules* **1984**, *17*, 2925.
- Lodge, T. P.; McLeish, T. C. B. *Macromolecules* **2000**, *33*, 5278.
- Haley, J. C.; Lodge, T. P. *Colloid Polym. Sci.* **2004**, *282*, 793.
- Haley, J. C.; Lodge, T. P. *J. Rheol.* **2004**, *48*, 463.
- Forrey, C.; Koberstein, J. T.; Pan, D. H. *Interface Sci.* **2003**, *11*, 211.
- Jones, R. A. L.; Kramer, E. J.; Rafailovich, M. H.; Sokolov, J.; Schwarz, S. A. *Phys. Rev. Lett.* **1989**, *62*, 280.
- Kim, E.; Kramer, E. J.; Garrett, P. D.; Mendelson, R. A.; Wu, W. C. *Polymer* **1995**, *36*, 2427.
- Faldi, A.; Genzer, J.; Composto, R. J.; Dozier, W. D. *Phys. Rev. Lett.* **1995**, *74*, 3388.
- Genzer, J.; Composto, R. *Macromolecules* **1998**, *31*, 870.
- Kim, E.; Kramer, E. J.; Osby, J. O.; Walsh, D. J. *J. Polym. Sci., Part B: Polym. Phys.* **1995**, *33*, 467.
- Kim, E.; Kramer, E. J.; Osby, J. O. *Macromolecules* **1995**, *28*, 1979.
- Composto, R. J.; Kramer, E. J.; White, D. M. *Polymer* **1990**, *31*, 2320.
- Flory, P. J. *Principles of Polymer Chemistry*; Cornell University Press: Ithaca, NY, 1953.
- Coleman, M. M.; Graf, J. F.; Painter, P. C. *Specific Interactions and the Miscibility of Polymer Blends*; Technomic: Lancaster, PA, 1991.
- Hino, T.; Song, Y. H.; Prausnitz, J. M. *Macromolecules* **1995**, *28*, 5717.
- Sferrazza, M.; Jones, R. A. L.; Bucknall, D. G. *Phys. Rev. E* **1999**, *59*, 4434.
- Helfand, E.; Tagami, Y. *J. Chem. Phys.* **1972**, *56*, 3592.
- Genzer, J.; Faldi, A.; Composto, R. J. *J. Chem. Phys.* **1996**, *105*, 10134.
- Helfand, E. *Macromolecules* **1992**, *25*, 1676.
- Binder, K. *Monte Carlo and Molecular Dynamics Simulations in Polymer Science*; Oxford University Press: Oxford, 1995.
- Werner, A.; Schmid, F.; Müller, M. *J. Chem. Phys.* **1999**, *110*, 5370.
- Clarke, C. J.; Eisenberg, A.; LaScala, J.; Rafailovich, M. H.; Sokolov, J.; Li, Z.; Qu, S.; Nguyen, D.; Schwarz, S. A.; Strzhemechny, Y.; Sauer, B. B. *Macromolecules* **1997**, *30*, 4184.
- Dai, K. H.; Kramer, E. J. *Polymer* **1994**, *35*, 157.
- Kramer, E. J. *Physica B* **1991**, *173*, 189.
- Harton, S. E.; Stevie, F. A.; Ade, H. *Macromolecules* **2005**, *38*, 3543.
- Reynolds, B. J.; Ruegg, M. L.; Mates, T. E.; Radke, C. J.; Balsara, N. P. *Macromolecules* **2005**, *38*, 3872.
- Schwarz, S. A.; Wilkens, B. J.; Pudensi, M. A. A.; Rafailovich, M. H.; Sokolov, J.; Zhao, X.; Zhao, W.; Zheng, X.; Russell, T. P.; Jones, R. A. L. *Mol. Phys.* **1992**, *76*, 937.
- Shin, K.; Hu, X.; Zheng, X.; Rafailovich, M. H.; Sokolov, J.; Zaitsev, V.; Schwarz, S. A. *Macromolecules* **2001**, *34*, 4993.
- Genzer, J.; Composto, R. J. *Polymer* **1999**, *40*, 4223.
- Seec, O. H.; Kaendler, I. D.; Tolan, M.; Shin, M.; Rafailovich, M. H.; Sokolov, J.; Kolb, R. *Appl. Phys. Lett.* **2000**, *76*, 2713.
- Stamm, M.; Reiter, G.; Kunz, K. *Physica B* **1991**, *173*, 35.
- Amashta, I. A. K.; Sanchez, G. *Eur. Polym. J.* **1975**, *11*, 223.
- Ade, H.; Kilcoyne, A. L. D.; Tylliszczak, T.; Hitchcock, P.; Anderson, E.; Harteneck, B.; Rightor, E. G.; Mitchell, G. E.; Hitchcock, A. P.; Warwick, T. *J. Phys. IV* **2003**, *104*, 3.
- Kilcoyne, A. L. D.; Tylliszczak, T.; Steele, W. F.; Fakra, S.; Hitchcock, P.; Franck, K.; Anderson, E.; Harteneck, B.; Rightor, E. G.; Mitchell, G. E.; Hitchcock, A. P.; Yang, L.; Warwick, T.; Ade, H. *J. Synchrotron Radiat.* **2003**, *10*, 125.
- Friedrich, C.; Schwarzwaelder, C.; Riemann, R.-E. *Polymer* **1996**, *37*, 2499.
- Pomposo, J. A.; Mugica, A.; Areizaga, J.; Cortazar, M. *Acta Polym.* **1998**, *49*, 301.
- Fetters, L. J.; Lohse, D. J.; Milner, S. T.; Graessley, W. W. *Macromolecules* **1999**, *32*, 6847.
- Helfand, E.; Sapse, A. M. *J. Chem. Phys.* **1975**, *62*, 1327.
- Russell, T. P. *Macromolecules* **1993**, *26*, 5819.
- Sferrazza, M.; Xiao, C.; Jones, R. A. L.; Bucknall, D. G.; Webster, J.; Penfold, J. *Phys. Rev. Lett.* **1997**, *78*, 3693.
- Fredrickson, G. H.; Sides, S. W. *Macromolecules* **2003**, *36*, 5415.
- Broseta, D.; Fredrickson, G. H.; Helfand, E.; Leibler, L. *Macromolecules* **1990**, *23*, 132.
- Shull, K. R.; Kramer, E. J. *Macromolecules* **1990**, *23*, 4769.
- Zheng, X.; Rafailovich, M. H.; Sokolov, J.; Y, S.; Schwarz, S. A.; Sauer, B. B.; Rubinstein, M. *Phys. Rev. Lett.* **1997**, *79*, 241.
- Zheng, X.; Sauer, B. B.; Alsten, J. G. V.; Schwarz, S. A.; Rafailovich, M. H.; Sokolov, J.; Rubinstein, M. *Phys. Rev. Lett.* **1995**, *74*, 407.
- White, D. M.; Nye, S. A. *Macromolecules* **1984**, *17*, 2643.
- Odian, G. *Principles of Polymerization*, 4th ed.; John Wiley & Sons: Hoboken, NJ, 2004.
- Munoz-Bonilla, A.; Madruga, E. L.; Fernandez-Garcia, M. *J. Polym. Sci., Part A: Polym. Chem.* **2005**, *43*, 71.
- Miwa, Y.; Tanabe, T.; Yamamoto, K.; Sugino, Y.; Sakaguchi, M.; Sakai, M.; Shimada, S. *Macromolecules* **2004**, *37*, 8612.
- Fuchs, K.; Friedrich, C.; Weese, J. *Macromolecules* **1996**, *29*, 5893.

MA051595R